Draft version December 20, 2023
Typeset using LaTeX **preprint** style in AASTeX631

Stellar Structure Simulation of ZAMS star of 1.35$M_\odot$ and Solar Composition

Jack Ford

(Dated: December 20th 2023)

1. INTRODUCTION

Stellar structures and processes are analytically complex and this dynamic system with many interacting parts naturally makes modeling the physical properties of a star a challenge. Thus, with advances in computing technology numerical methods and modeling have proven to be a useful tool for studying the processes within stellar interiors. The goal of this project was to create a ZAMS model that, given the mass and metallicity of a star, would be able to model the structure and dominant processes within the star and return observables that when compared with real data could reveal insight into what kind of object is being observed. Built in python using functions of stellar structure equations (mainly from Kippenhahn et al. (2012) and Hansen et al. (2004)) along with numerical integration and iterative optimization from packages such as SciPy, a virtual model of the chosen star is generated and is proven here to be highly accurate when compared to state-of-the-art software in the field such as Modules for Experiments in Stellar Astrophysics (MESA)(Paxton et al. 2011).

2. DESCRIPTION OF THE MODEL

First the inputs to the model are the mass and elemental abundances of the ZAMS star. The chosen star is of mass 1.35 solar masses($M_\odot$) and solar abundances, ie. X=0.7, Y=0.28, Z=0.02. The stellar parameters used as a guess to initialize the model and that we optimize for are the radius(R_f), luminosity(L_f), central pressure(P_c), and core temperature(T_c), which will be described later in this section.

$$M_r = \int_0^r 4\pi r^2 \rho(dr) \tag{1}$$

The structure and interior of the star are governed by the four following coupled differential equations with respect to the Lagrangian mass coordinate, which itself is defined by Equation(1). Integrating these equations over the total 1.35($M_\odot$) of the star will then yield the pressure, luminosity, radius, and temperature as a function of mass, which is much more practical in stellar modelling as the radial profile of stars differ greatly as the total mass changes. It is important to note, as discussed in Hansen et al. (2004), these equations hold for a non-rotating ZAMS star in hydro-static equilibrium and do not consider the effects of external forces like magnetic fields, which are too computationally intense to be investigated in this project.

Corresponding author: Jack Ford jford51@jh.edu

$$\frac{dl}{dm} = \epsilon \tag{2}$$

$$\frac{dP}{dm} = \frac{-Gm}{4\pi r^4} \tag{3}$$

$$\frac{dr}{dm} = \frac{1}{4\pi r^2 \rho} \tag{4}$$

$$\frac{dT}{dm} = \frac{-GmT}{4\pi r^4 P}\nabla \tag{5}$$

A ZAMS star is also chemically homogeneous, and under the assumption that the star is completely ionized, the mean molecular weight of the star is uniform throughout and follows Equation(6). We can also assume that for each Lagrangian mass shell, the star is in thermodynamic equilibrium or local thermodynamic equilibrium closer to the surface. This means the radiation temperature is in equilibrium with the gas temperature and the equation of state can be written as follows(7),

$$\mu = \frac{4}{3+X} \tag{6}$$

$$P_{tot} = P_{gas} + P_{rad} = \frac{\rho N_A k T}{\mu} + \frac{aT^4}{3} \tag{7}$$

where the pressure at any point is the sum of the ideal gas pressure and the radiation pressure, N_A is Avogadro's number, k is the Boltzmann constant, and $a = \frac{4\sigma}{c}$ is the radiation constant.

The temperature gradient(∇) seen in Equation(5) is determined by whether or not the region of the star being integrated over is convective or radiative. The adiabatic temperature gradient is given by (8) , which for an ionized monatomic gas is ($\frac{2}{5}$) or 0.4. The radiative temperature gradient is given by (9). When the radiative temperature gradient is steeper or greater than the adiabatic gradient, energy transport is driven by convection, and when the adiabatic gradient is greater than that region of the star is radiative. As the adiabatic gradient remains constant, calculating the correct radiative gradient, which itself relies heavily on the opacity, pressure, luminosity, and temperature at each point, is paramount to achieving an accurate model.

$$\nabla_{ad} = [\frac{d(lnT)}{d(lnP)}]_{ad} = \frac{\gamma - 1}{\gamma} = \frac{2}{5} \tag{8}$$

$$\nabla_{rad} = [\frac{d(lnT)}{d(lnP)}]_{rad} = \frac{3}{64\pi\sigma G} * \frac{\kappa P l}{m T^4} \tag{9}$$

The Rosseland mean opacity(κ), as seen in the calculation of the radiative temperature gradient, determines how easily photons can travel through the star before being absorbed. Understandably

this is an incredibly important parameter in stellar astrophysics but extremely difficult to calculate analytically or numerically as it is dependent on a number of factors, chief among them being density and temperature. However there exist a number of tabulated opacities from past nuclear physics studies, and in this project, we use OPAL tables generated by Lawrence Livermore National Laboratory and discussed in further detail by Iglesias & Rogers (1996). The table chosen has solar composition and abundances, as the project requires, and given a density and temperature is able to return an opacity. Using the SciPy interpolation package, this table is able to provide an opacity at any point within the star as the mass, density, and temperatures fall well within the bounds. Thus, the radiative and convective structure of the star is able to be completely and accurately characterized by the model.

The energy generation and source of luminosity comes from the nuclear reactions at the core of the star. Given a mass of $1.35(M_\odot)$, hydrogen fusion in the form of both the pp-chain and the CNO cycle contribute to energy generation. An analytical fit to measured and tabulated values for the energy output of the pp-chain as given in Ch. 18 of Kippenhahn et al. (2012) is given by Equation (10), where $\psi \approx 1.2$ based on the estimated core temperature and helium composition.

$$\begin{aligned} \epsilon_{pp} &= 2.57 * 10^4 \psi f_{11} g_{11} X^2 T_9^2 * (e^{-3.381/T_9^{1/3}}) \\ g_{11} &= (1 + 3.82T_9 + 1.51T_9^2 + 0.144T_9^3 - 0.0114T_9^4) \end{aligned} \tag{10}$$

$$f = e^{E_D/kT}; \frac{E_d}{kT} = 5.92 * 10^{-3} Z_1 Z_2 \sqrt{\frac{\rho\zeta}{T_7^3}} \tag{11}$$

The weak screening factor considers the repulsive electrostatic forces of given atoms in relation to the temperature and provides an additional limiting term to the pp-chain output. This factor follows the form of Equation (11), where $Z_1 = Z_2 = 1$ for hydrogen fusion and $\zeta \approx 1$ for weak screening. For $T_7 \approx 1$, which the core of a mass $1.35(M_\odot)$ is roughly the same temperature, reactions with $Z_1 * Z_2 < 16$ need this weak screening correction. Since the CNO cycle dominates at higher temperatures and with higher $Z_1 * Z_2$, this factor becomes negligible.

$$\begin{aligned} \epsilon_{CNO} &= 8.24 * 10^{25} g_{14,1} (0.7 * Z) X \rho T_9^{-2/3} e^{-15.231 * T_9^{-1/3} - (T_9/0.8)^2} \\ g_{14,1} &= (1 - 2.00T_9 + 3.41T_9^2 - 2.43T_9^3) \end{aligned} \tag{12}$$

The energy generation rate for the CNO cycle is given by Equation(12). The total energy generation within the core of the star is then both these rates summed together.

3. BOUNDARY CONDITIONS

For the model to properly initialize, the correct boundary conditions for the ZAMS star need to be considered. The center and the surface of the star pose singularities in the equations above that when solved numerically would break down. Thus, proper approximations must be made to ensure the accuracy of the numerical integration.

3.1. *The Center*

At the center of the star, $m = 0$, $r = 0$, and $l = 0$, however these zeroes cannot be propagated through the integration, so a starting point in the mass coordinate of m = 1e-5M is chosen, as Section 11.1 of Kippenhahn et al. (2012) suggests. This allows us to use the integral of the differential equations above in the limit of $m \to 0$, which analytically is possible to solve and is given in 11.1 of Kippenhahn et al. (2012) as the follows. These equations provide us all the necessary starting points for integration from the center out, given only initial guesses for the central temperature and pressure.

$$\begin{aligned} r &= (\frac{3m}{4\pi\rho_c})^{1/3} \\ l &= \epsilon(T_c, \rho_c) * m \\ P &= P_c - [\frac{3G}{8\pi} * (\frac{4\pi\rho_c}{3})^{4/3} * m^{2/3}] \\ T &= T_c \end{aligned} \tag{13}$$

3.2. *The Surface*

At the surface of the star the other two stellar parameters, pressure and temperature, would seem to tend to zero or whatever the pressure and temperature of the immediate space surrounding the star might be. However, this is not the case and the transition is much more gradual, resulting in an incorrect model. To correctly identify the surface, the definition of the stars photosphere is used where the optical depth $\tau = 2/3$. Relating optical depth to the surface gravity of the star yields the following equation for surface pressure below. The term $\bar{\kappa}$ is the mean opacity of the stellar atmosphere which can be numerically calculated, but for solar like stars can also be approximated to be $\bar{\kappa} \approx 0.3$. At the same optical depth, defining the star to be a blackbody with the following formula will yield the surface temperature.

$$P_R = \frac{2GM}{3R^2}\frac{1}{\bar{\kappa}} \tag{14}$$

$$T_{eff} = (\frac{L}{4\pi\sigma R^2})^{1/4} \tag{15}$$

4. NUMERICAL METHODS

4.1. *Integration and Optimization*

Numerical integration on the 4 stellar structure differential equations was done using the Scipy integration package, specifically the solve_ivp function with uses the Runge-Kutta method to numerically integrate from the starting point near the center of the star (using the central boundary conditions given above) to the halfway point at m=1/2M. A second identical integration starting from the surface boundary and ending at the halfway point is also performed. The 4 parameters needed to initialize the integration and calculate the boundary conditions are stellar radius, stellar luminosity, central pressure, and central temperature (R_f, L_f, P_c, T_c). Integrated over a total of 4000

mass cuts, the two integrations are contained within the shootf function, the output of which are the radius, luminosity, pressure, and temperature as a function of mass within the star. Plotting the outputs then reveals a graphical interpretation of the stellar interior.

The shootf function alone will provide a working model of a stellar interior, however based on the initial inputs there is no guarantee that the model will be accurate or even converge at the midpoint. Therefore, an iterative approach to finding and updating the optimal stellar parameters is needed. The shootf function would generate a model given an initial guess, the least square difference between the midpoints for each parameter was calculated, and then this single value was minimized using the least_squares function from the SciPy optimization package. This function would update the initial R_f, L_f, P_c, T_c, in order to minimize the loss function, thus converging on the final stellar parameters and a model that satisfies the 4 differential equations as well as the boundary conditions.

4.2. *Initial Guesses*

The initial guesses used to initialize the optimization are all near solar values, as a $1.35(M_\odot)$ star has similar processes and structures within its core and envelope. Therefore, a solar radius and solar luminosity were used, as well as the solar central pressure and temperature which are recorded on a NASA GFSC fact sheet (Williams 2022). There is a great computational advantage to using solar values as initial guesses, as the optimization function can be modified to take floating point values near that of unity as an input, which are then be scaled up to values in cgs units and fed into the shootf function. This allows the scaled calculated difference at the midpoint to be values much more manageable, reducing the computation time and number of iterations needed significantly.

	Scaled Parameters	Absolute Values
R_f	1.45	$1.008 * 10^{11}$ cm
L_f	2.85	$1.094 * 10^{34}$ erg s^{-1}
P_c	0.95	$1.824 * 10^{17}$ dyne cm^{-2}
T_c	1	$1.571 * 10^{7}$ K

Table 1. The initial parameters that are input into the shootf function are the absolute values, which are obtained by multiplying solar values by the scaled parameters.

In addition, the loss function proved to have many local minima, so careful tweaking of the 4 parameters was needed in order to find a guess that would converge to the global minimum. Scaled inputs made this task much easier, as tweaking multiple ratios near order unity is much simpler than changing cgs values on the order of 1e10. Given more time, a 4D scan of initial guesses within set bounds could be made as a more automated and optimal approach to finding the global minimum of the loss function and thus the optimal stellar parameters.

5. RESULTS AND COMPARISON

Figure 1 shows the results of the numerical integration given the chosen scaled initial guess. Clearly these are not the correct parameters of R_f, L_f, P_c , and T_c as there are noticeable discrepancies at the midpoint of each calculation. Following the optimization, at a cost of 6.8e-13 and after only 21

iterations the model converged as seen in figure 3. The optimal stellar parameters are shown in Table 2. Given this final model we have now defined r, l, P, T in the Lagrangian mass coordinates for any point within the star, which yields accurate constraints on information like the convective radiative boundary, density, and temperature gradients within the interior.

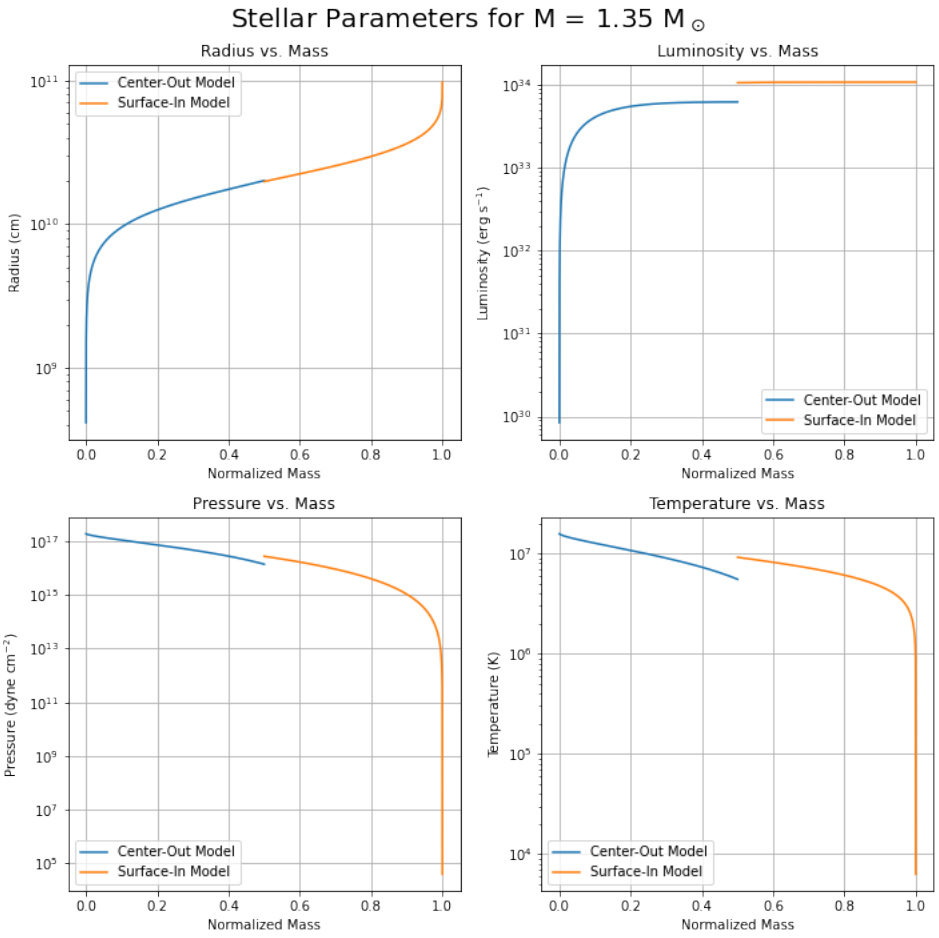

Figure 1. Center Out and Surface In calculations plotted for each of the 4 stellar parameters as a function of mass.

	Scaled Parameters	Absolute Values
R_f	1.43	$9.945 * 10^{10}$ cm
L_f	2.80	$1.074 * 10^{34}$ erg s^{-1}
P_c	1.02	$1.973 * 10^{17}$ dyne cm^{-2}
T_c	1.08	$1.701 * 10^{7}$ K

Table 2. The optimized parameters that are obtained from iterating the shootf function with least_squares. The scaled parameters are what is returned by the optimizer and multiplying by solar values yields the respective absolute values.

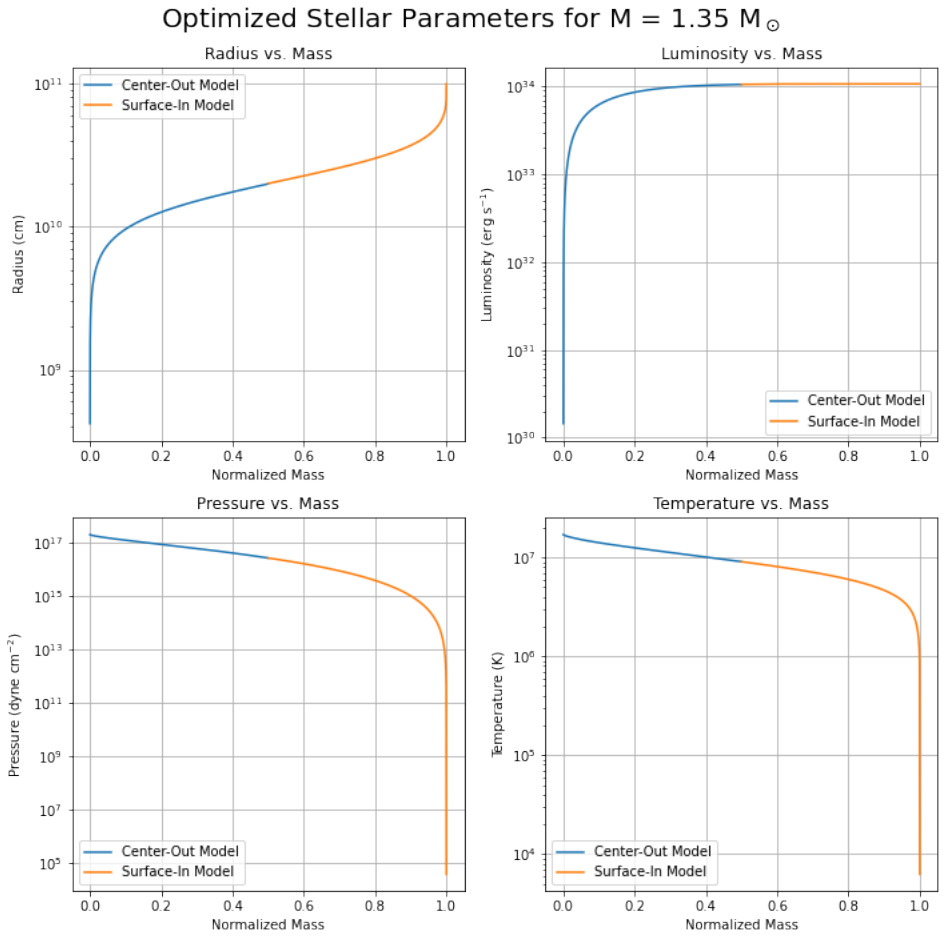

Figure 2. Same plots as Figure 1, however R_f, L_f, P_c, T_c have been optimized, removing the discrepancy at the mass midpoint.

The results obtained above can be compared to the state-of-the-art stellar modeling software MESA, which is capable of reproducing the same parameters and plots above for ZAMS stars given only the stellar mass and composition. Comparing the two is indeed encouraging, as Table 3 shows the percent difference between each parameter is extremely low. As a result, the plots of the star interior are identical and plotted directly on top one another.

	MESA Values	Percent Difference
R_f	$9.191 * 10^{10}$ cm	8.21%
L_f	$1.077 * 10^{34}$ erg s^{-1}	0.30%
P_c	$1.925 * 10^{17}$ dyne cm^{-2}	2.44%
T_c	$1.609 * 10^{7}$ K	0.65%

Table 3. The parameters MESA yields compared to the results above using the percent difference.

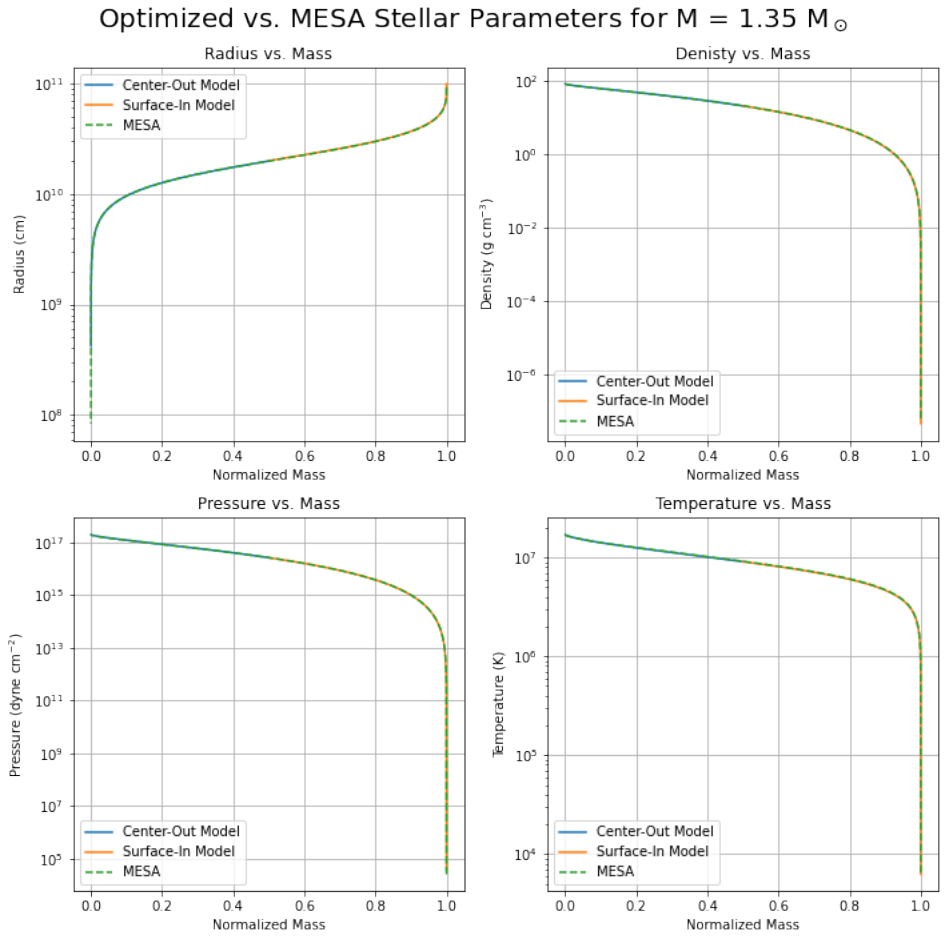

Figure 3. Same plots as Figures 1 and 3 now with the MESA results plotted alongside (or rather on top).

6. CONCLUSIONS

In conclusion, the stellar structure modelling script created is proven to provide accurate models and observables for near solar mass stars given only the mass and composition. This program can not cover as broad a range of star as MESA, as this project was designed with the intent of modeling a specific star and thus tools like the opacity table, energy generation rates, boundary conditions, initial guesses, etc would all need to be updated. However, given the range of mass that this program can operate within, it is successfully shown to be as reliable as the state of the art for stellar astrophysical simulation.

ACKNOWLEDGEMENTS

I would like to thank Professor Kevin Schlaufman for an amazing quarter and interactive class, which was crucial to my understanding of the stellar structure equations and processes used in this project. I would also like to thank my classmates whose collaboration on debugging code cured many a headache over the time spent on this project.

REFERENCES

Hansen, C. J., Kawaler, S. D., & Trimble, V. 2004, Stellar interiors : physical principles, structure, and evolution., 2nd edn., Astronomy and astrophysics library (New York: Springer)

Iglesias, C. A., & Rogers, F. J. 1996, ApJ, 464, 943, doi: 10.1086/177381

Kippenhahn, R., Weigert, A., & Weiss, A. 2012, Astronomy and Astrophysics Library, doi: 10.1007/978-3-642-30304-3

Paxton, B., Bildsten, L., Dotter, A., et al. 2011, ApJS, 192, 3, doi: 10.1088/0067-0049/192/1/3

Williams, D. R. 2022, Sun fact sheet, NASA. https://nssdc.gsfc.nasa.gov/planetary/factsheet/sunfact.html